Journal of Magnetic Resonance 208 (2011) 204–209

Contents lists available at ScienceDirect

Journal of Magnetic Resonance

journal homepage: www.elsevier.com/locate/jmr

Spontaneous emission of NMR signals in hyperpolarized proton spin systems

Hsueh-Ying Chen, Youngbok Lee, Sean Bowen, Christian Hilty *

Center for Biological NMR, Department of Chemistry, Texas A&M University, College Station, TX 77843, USA

ARTICLE INFO

Article history:
Received 12 August 2010
Revised 27 October 2010
Available online 11 November 2010

Keywords:
Hyperpolarization
Radiation damping
NMR MASER
Spin temperature
Dynamic nuclear polarization

ABSTRACT

Hyperpolarization of nuclear spins is gaining increasing interest as a tool for improving the signal-to-noise ratio of NMR and MRI. While in principle, hyperpolarized samples are amenable to the same or similar experiments as are used in conventional NMR, the large spin polarization may give rise to unexpected effects. Here, spontaneous emission of signal was observed from proton spin systems, which were hyperpolarized to negative spin temperature by dynamic nuclear polarization (DNP). An unexpected feature of these emissions is that, without any radio-frequency excitation, multiple beats arise that cannot be explained by the Bloch equations with radiation damping. However, we show that a simple modification to these equations, which takes into account an additional supply of hyperpolarized magnetization from a reservoir outside of the active detection region, can phenomenologically describe the observed signal. The observed effect demonstrates that even well-known mechanisms of spin evolution can give rise to unexpected effects when working with hyperpolarized samples, which may need to be addressed through the development of new experimental techniques.

1. Introduction

Hyperpolarization of nuclear spins is gaining considerable momentum for the enhancement of the signal in magnetic resonance, with applications ranging from medical imaging to high-resolution spectroscopy of chemical compounds. In the widespread application of hyperpolarization, however, it is often overlooked that due to the highly polarized spin system, effects not commonly encountered in conventional NMR spectroscopy need to be considered. Such effects include phenomena related to the emission or absorption of spin noise that have been previously described using thermal polarization [1–3], but may become more prominent in hyperpolarized samples. Desvaux et al. [4] have shown that ^{129}Xe, hyperpolarized by optical pumping, can enhance the absorption of noise at the Larmor frequency of that nucleus. Recently, the same phenomenon has been observed by Giraudeau et al. [5] using hyperpolarized ^{1}H nuclei. However, when a sample is polarized to negative spin temperature, an unusual and chaotic behavior arises, where a series of beats of NMR signal can be observed under certain conditions. The physical origin of such spontaneous emissions has been attributed to interplay between radiation damping and the effect of distant dipolar fields. In the absence of radio-frequency pulses, it has been proposed that the emission of such bursts may be triggered by random spin noise [6]. These emissions therefore arise from positive feedback through coupling with the resonant detection coil circuit, and are different from the previously observed spontaneous emissions of signal from a saturated spin system with zero polarization [2]. The observation of noise triggered spontaneous emission is highly dependent on the conditions used, and it has also been noted that observation of multiple signal emissions in hyperpolarized samples of ^{1}H is less likely due to the shorter relaxation time [5] and the higher gyromagnetic ratio [6].

With the recent development of various technologies for dynamic nuclear polarization (DNP), it has become commonplace to polarize many different nuclei. Of particular importance is ^{1}H, the NMR active nucleus with highest abundance. Due to the large signal enhancement provided by DNP (on the order of 10^{2}–10^{4} as compared to thermally polarized spins), applications of this technique in traditional areas of NMR spectroscopy, such as analytical and organic chemistry, are forthcoming. In this context, it may be interesting to investigate in more detail the non-canonical behavior that hyperpolarized spin systems can exhibit. Here, we show that the spontaneous emission of multiple beats of NMR signal could be observed for ^{1}H nuclei when the spin system has been hyperpolarized to a negative spin temperature and the sample is injected into an NMR spectrometer for measurement. We examine the conditions under which this phenomenon can be observed, rationalize the appearance of these emissions, and discuss their implications for the application of hyperpolarized spectroscopy.

2. Materials and methods

2.1. Hyperpolarization

The optimal frequencies for DNP polarization were determined by measuring the frequency dependence of the NMR signal in the

* Corresponding author.
E-mail address: chilty@chem.tamu.edu (C. Hilty).

1090-7807/$ - see front matter © 2010 Elsevier Inc. All rights reserved.
doi:10.1016/j.jmr.2010.11.002

solid state (Fig. 1) [7]. To accomplish this, a sample of 10% H_2O, 40% D_2O and 50% DMSO-d_6 containing 15 mM free radical, 4-Hydroxy-2,2,6,6-tetramethylpiperidine 1-oxyl (TEMPOL, Sigma Aldrich, St. Louis, MO) was irradiated for 60 s at each of 66 frequencies between 93.66 GHz and 94.31 GHz. The irradiation frequency was verified using a frequency counter (EIP 578B, Phase Matrix, San Jose, CA). NMR spectra were measured using the detection coil in the HyperSense DNP polarizer (Oxford Instruments, Tubney Woods, UK) and a separate 400 MHz NMR console (Bruker, Billerica, MA). The resulting series of free induction decays (FID) was Fourier transformed, and the frequency profile was generated by integration of each spectrum.

For hyperpolarized NMR spectroscopy, samples of dimethyl sulfoxide (DMSO) were prepared in H_2O (1:1 v/v) mixtures with 15 mM TEMPOL and 1 mM gadolinium diethylene triamine pentaacetic acid (Gd-DTPA, Sigma Aldrich, St. Louis, MO). 20 μl of the sample was polarized for 30 min, at a temperature of 1.4 K, using mm-waves of 100 mW power at the frequencies corresponding to positive or negative spin temperature (see Results and discussion). Subsequently, 4 mL of deuterium oxide (Cambridge Isotope Laboratories, Andover, MA) at ~160 °C and 10 bar pressure was used to dissolve and carry the hyperpolarized sample into a sample injector device. The first 500 μL of the liquid was injected into a 5 mm NMR tube that was pre-installed in the NMR spectrometer, using nitrogen gas at a forward pressure of 1.8 MPa, against a backpressure of 1.0 MPa to prevent outgassing [8]. The final concentration of hyperpolarized analyte in the NMR tube was estimated to be 115 mM DMSO and 453 mM H_2O.

2.2. NMR spectroscopy

The coil of a high-resolution 400 MHz NMR probe (Bruker, Billerica, MA) was tuned using the procedure described in [9], so that the resonance frequency of the reception circuit matches the Larmor frequency. The magnetic field was shimmed to a homogeneity <2.5 ppb using a sample of identical volume and composition prior to the experiment. Single NMR scans were acquired either with or without prior application of a $\pi/2$ radio-frequency (RF) pulse. Measurements without RF pulse were triggered at the start of sample injection, prior to the arrival of the polarized solution in the NMR tube. Measurements with RF pulse were initiated 815 ms after the start of sample injection, to ensure a sufficient amount of time for sample injection and stabilization. The total experimental time was 190 s, during which 1201922 complex data points were acquired. All measurements from hyperpolarized sample were carried out without the use of a lock system. Time–frequency analysis was performed by a Fast Fourier Transform (FFT) of data contained in a sliding window of 256 complex points in length. Data processing and plotting was done in the program MATLAB (MathWorks Inc., Natick, MA). The actual timing of sample delivery (time points A and B in Fig. 2, for the start and end of arrival of sample in the NMR tube, respectively) was determined on a sample outside of the NMR magnet, using a camera. T_1 relaxation times under the experimental conditions used for the DNP experiments were estimated from hyperpolarized samples with positive spin temperature using a sequence of small flip angle excitations [10,11], as well as from inversion recovery experiments.

For reference, the radiation damping time constant was measured in a non-hyperpolarized sample of 95% DMSO and 5% D_2O in the 400 MHz NMR spectrometer. An inversion recovery experiment was applied as described in [12], and the equation

$$M_z = M_z^{eq}\tanh[R_{rd}(t - t_0)] \quad (1)$$

was fitted to the experimental data. Here, M_z^{eq}, R_{rd} and t_0 are the initial thermal magnetization in the z direction, the radiation damping rate, and the latency interval, respectively.

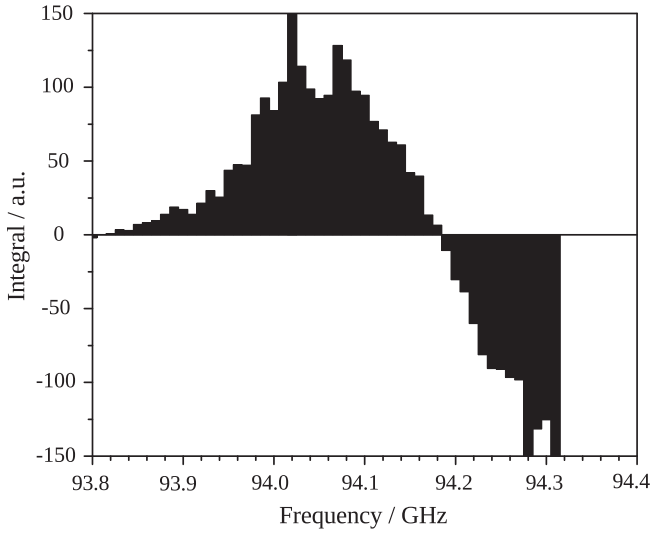

Fig. 1. Dependence of solid-state ^1H polarization on microwave frequency for a sample of 10% H_2O/40% D_2O/50% DMSO-d_6 containing 15 mM TEMPOL free radical. Spurious points of large intensity (clipped in the figure) are likely due to arcing of the NMR coil immersed in liquid helium.

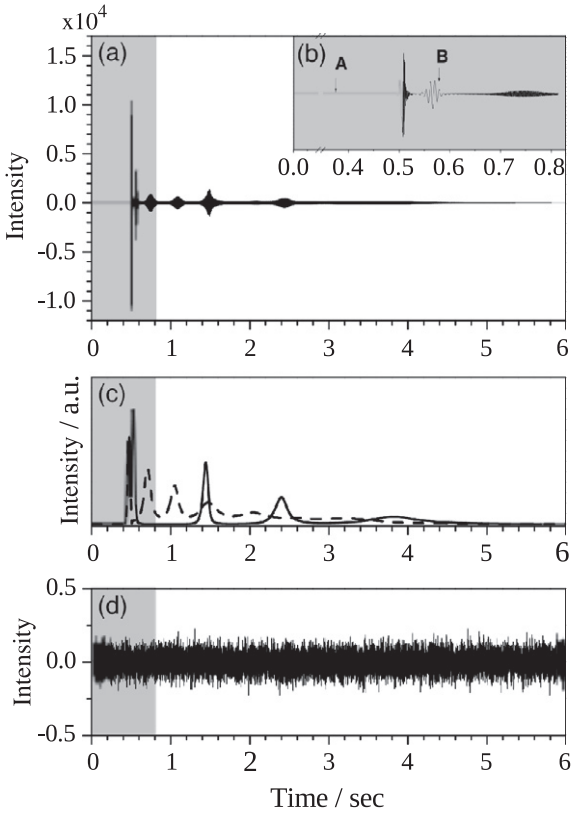

Fig. 2. (a) Signals from a sample of DMSO/H_2O (1:1 v/v) polarized to negative spin temperature and dissolved in D_2O. (b) Inset: expanded view of the signal in the time window from 0 to 815 ms. The time point $t = 0$ is the point of triggering of the injection valve. The sample starts arriving in the NMR tube at time point A, and tube is completely filled at time point B. (c) The corresponding time–frequency analysis of FID (a) was performed by a FFT of data contained in a sliding window of 256 complex points in length (time window of 40 ms). The peak height of the spectra was plotted as a function of time. The solid and dashed lines refer to H_2O and DMSO signals, respectively. (d) The hyperpolarized sample of DMSO/H_2O (1:1 v/v) with positive temperature was dissolved by D_2O and measured under early triggered acquisition mode, showing no signals inside the blind time (grey area: the time before the sample injection and stabilization in the normal measurement, ~815 ms).

Numerical solutions of radiation damping equations were obtained using the program Mathematica (Wolfram Research, Champaign, IL).

3. Results and discussion

3.1. Hyperpolarization to negative spin temperature

Using DNP in the solid state, spin systems with positive or negative spin temperature are readily produced [13]. Fig. 1 shows the frequency dependence of polarization, recorded within the frequency range accessible by the microwave source used. The intensity maximum at 94.005 GHz corresponds to polarization with positive spin temperature, where the majority of spins are aligned parallel with the magnetic field, and the negative intensity maximum at 94.270 GHz corresponds to the negative spin temperature, where the majority of spins are aligned anti-parallel with the magnetic field. It can also be noted that the frequency difference between the maxima is 265 MHz, which indicates that the DNP polarization process under the conditions used (see Materials and methods) takes place via a multi-electron process [14].

DNP polarized samples were dissolved and injected into the NMR spectrometer in order to analyze their NMR signal. In the archetypal pulsed NMR experiment, a single $\pi/2$ radio-frequency pulse would be applied to a tuned coil surrounding the sample, and the resulting free induction decay (FID) would be observed. This experiment was used in order to estimate the level of polarization obtained, by comparison with a spectrum acquired in the same spectrometer using a thermally polarized sample. For the DMSO signal, a typical polarization level of ca. 4% is achieved, corresponding to a signal enhancement of approximately 1300 as compared to the thermal polarization in the field of the 400 MHz NMR spectrometer.

3.2. Spontaneous signal emission

For a hyperpolarized sample with negative spin temperature, spontaneous emission of signals is readily observed as soon as the sample is introduced into the active region of an NMR coil, even in the absence of RF pulses. Fig. 2 shows such emissions from a mixture of DMSO and H_2O, which was hyperpolarized on proton spins, and dissolved in deuterium oxide (D_2O) before injection into the NMR detection coil. Since the NMR experiments measuring spontaneous emission do not require a radio-frequency pulse, data acquisition was initiated before the solution arrived in the NMR spectrometer, in order to detect all potential signals. The grey areas in Fig. 2 designate the time for sample injection and stabilization that would normally elapse before the start of an NMR experiment.

The data in Fig. 2a and b indicate the emission of strong, recurring signals, starting almost immediately after the arrival of polarized solution in the detection coil. In order to distinguish the identity of the sample constituents giving rise to the different recurring signals, a time–frequency analysis was performed by a sliding Fourier transform. The resulting peak intensity at the chemical shifts corresponding to H_2O and DMSO is plotted in function of time in Fig. 2c. Due to substantial inhomogeneity during sample injection, the intensities obtained for the grayed time window (0–815 ms) may not be quantitative, and the signals appear less regular. Nevertheless, in Fig. 2b the appearance of signals with different frequency stemming from water and DMSO protons can be seen. After this time, the sample has settled, and the line width in the spectra obtained with sliding Fourier transform remains constant, since the true line width had fallen below the frequency resolution given by the window used for the Fourier transform. From Fig. 2 it can however be seen that the recurring beats become longer in duration at larger time. From this observation, it can be inferred that the true line width decreases with each emission. The time–frequency representation of the signal shows multiple emissions both from H_2O and DMSO spins. Presumably due to chaotic processes during sample injection, if the experiment is repeated under identical conditions, the appearance of the signal can vary. However, in all experiments that were carried out, the signal between two consecutive recurrences was nonzero and the intensity of a later recurrence was smaller than that of an earlier one. In Fig. 2d, the measurement of a sample hyperpolarized to positive spin temperature serves as a control experiment. The absence of coherent signal excludes the possibility that the spin emission from the other samples is due to influences unrelated to the spin system, such as electronic interferences or external excitation of the detection circuit during sample injection.

3.3. Radiation damping

Coherent emissions in the form of radiation damping are common from solvent signals in high-resolution NMR spectroscopy. A typical signal from radiation damping arises shortly after generating the inverted spin state in the NMR coil, and is characterized by a rising, then falling signal amplitude [15]. In typical NMR experiments, radiation damping is triggered by a small amount of transverse magnetization that is present in the sample following a non-ideal π inversion pulse. The coupling of spin magnetization to the tuned detection coil of the NMR receiver can be described semi-classically by modified Bloch equations [6,16–18] as shown below.

$$\frac{dM_T}{dt} = -\frac{M_T}{T_2^*} - \frac{M_T M_z}{M_0 \tau_{rd}}, \tag{2}$$

$$\frac{dM_Z}{dt} = -\frac{M_z}{T_1} + \frac{M_T^2}{M_0 \tau_{rd}}, \tag{3}$$

Here, M_0 is length of the initial magnetization vector, which is aligned with the direction of the magnetic field (z-direction), and τ_{rd} is the characteristic radiation damping time. M_z is the magnetization in the longitudinal direction, and $M_T = \sqrt{M_x^2 + M_y^2}$ is the magnitude of transverse magnetization. Since in the hyperpolarized experiment the magnetization at thermal equilibrium is much smaller than the initial magnetization, $M_{eq} \ll M_0$, it is neglected in Eq. (3). In order to compare the observed signal to a radiation damping model, the magnetization $M_{\alpha,815\mathrm{ms}}$ and $M_{\beta,815\mathrm{ms}}$ of the hyperpolarized DMSO spin system with positive and negative spin temperature, respectively, was estimated by applying a $\pi/2$ pulse at $t \sim 815$ ms after the start of sample injection. It was found that $M_{\beta,815\mathrm{ms}}/M_{\alpha,815\mathrm{ms}} = 0.4$. Since the solid-state polarization levels (Fig. 1) for polarization to positive and negative spin temperature are similar, this observation implies that the initial magnetization $M_{\beta,0}$ decays more rapidly than the initial $M_{\alpha,0}$, presumably due to radiation damping.

The characteristic radiation damping time constants of polarized samples were estimated by comparison to a measurement of radiation damping in a thermally polarized reference sample of DMSO (see Materials and methods). From fitting of the data obtained with the non-hyperpolarized reference sample, the radiation damping rate (R_{rd}) and the latency interval (t_0) were determined to be 23 s^{-1} and 0.048 s, respectively.

The radiation damping rate can also be expressed as

$$R_{rd} = \frac{1}{\tau_{rd}} = \frac{\mu_0}{2} \eta Q |\gamma M_0|, \tag{4}$$

where μ_0, η, Q, γ, M_0 are the vacuum permeability, the filling factor and the quality factor of the probe, the gyromagnetic ratio, and the initial magnetization, respectively [6]. This equation can be used to

infer the radiation damping rate for other samples, if the relative sample magnetizations are known. For DMSO, this ratio was estimated to be 12.5, by comparing the intensities obtained by applying a $\pi/2$ pulse to the thermally polarized reference sample and to a hyperpolarized sample, respectively. According to Eq. (4), the radiation damping rate of the hyperpolarized sample is therefore 275 s^{-1}. For water, the rate is of the same order in magnitude; however the exact number is more difficult to determine due to the possibility of the presence of residual non-polarized water in the dissolution solvent, which would affect the estimate of the absolute polarization level. Not surprisingly, the radiation damping is more significant in the hyperpolarized sample, even though the spin concentration is two orders of magnitude lower than in the thermally polarized reference sample.

3.4. Origin of multiple emissions

Radiation damping appears to be the most reasonable explanation for the observed emission of signals. However, the Bloch equations with radiation damping (Eqs. (2) and (3)) can describe only one single emission, where the observed signal rises, then falls. For illustration, a numerical solution of these equations using parameters close to the expected experimental conditions for a DMSO spin system is shown in Figs. 3a and b. This is in contrast to the present observation of multiple "beats" in the signal from samples that have been hyperpolarized to negative spin temperature, and subsequently injected into the NMR spectrometer.

In similar experiments conducted with hyperpolarized xenon, the occurrence of multiple MASER emissions has been attributed to a chaotic behavior of the spin system resulting from interplay between radiation damping and the effect of distant dipolar fields [17]. It was further apparent that in that case, individual emissions were independently triggered by spin noise. For the proton signal emission observed here, the situation appears to be different. The residual signal between the consecutive beats in our observation is always larger than the noise level (see Fig. 2). Therefore, in contrast to the observations with hyperpolarized xenon, in the present case it seems unlikely that emissions are triggered independently by noise originating from the spin system itself. However, the experimental conditions are different; in the present case the sample is injected into the NMR tube, and initial emissions appear already during the injection process. While, as stated above, the Bloch equations by themselves cannot describe the observed evolution of magnetization, it is noted that in experiments where hyperpolarization is used to generate a sustained MASER emission, for example for the purpose of magnetic field measurements, such transient oscillations are commonplace [18]. In those experiments, however, spins with negative spin temperature are continuously supplied to the system under observation.

Likewise, in the present case the signal oscillations observed can at least phenomenologically be explained by inclusion of an additional term in the Bloch equations in an attempt to describe a similar physical process:

$$\frac{dM_T}{dt} = -\frac{M_T}{T_2^*} - \frac{M_T M_z}{M_0 \tau_{rd}}, \tag{5}$$

$$\frac{dM_z}{dt} = -\frac{M_z}{T_1} + \frac{M_T^2}{M_0 \tau_{rd}} - \alpha e^{-t/\tau_a}, \tag{6}$$

In Eq. (6), the last term continuously supplies negative polarization from a reservoir not coupled to the coil. The parameter α indicates the initial rate of addition of magnetization, and τ_a is a time constant describing an exponential reduction in the rate of added magnetization as time progresses. The addition of magnetization during the initial time (between time points A and B in Fig. 2b) arises naturally due to the sample injection process, whereas the addition of magnetization at later times would be expected due to sample motions. Therefore, τ_a should be understood as an average parameter that includes all of these contributions. Specifically, τ_a would be dependent both on spin-relaxation in the volume outside of the active coil region, as well as on the rate of sample introduction.

Fig. 3 shows a numerical solution of Eqs. (2) and (3), which corresponds to the typical radiation damping process, as well as of the modified Eqs. (5) and (6). The parameters used are indicated in the figure caption. In these parameters, the relaxation times were

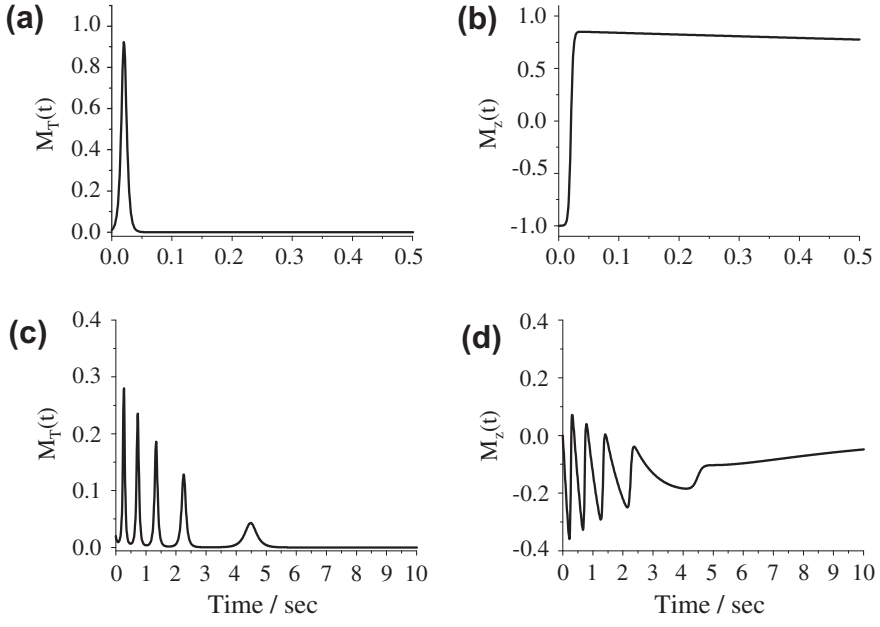

Fig. 3. Numerical solutions of Bloch equations. (a) and (b) transverse and longitudinal magnetization obtained from original Eqs. (2) and (3), (c) and (d) magnetization obtained from Eqs. (5) and (6), with inclusion of an additional term supplying negative polarization during the course of the experiment. Parameters were $T_2^* = 50$ ms, $T_1 = 5$ s, $\tau_{rd} = 3.6$ ms, $M_0 = 1$, $\alpha = 1$, $\tau_a = 1$ s. Boundary conditions were $M_T(0) = 0.01$ and $M_z(0) = -M_0$ for (a) and (b), and $M_T(0) = 0.01$ and $M_z(0) = 0$ for (c) and (d).

estimated from actual conditions for DMSO samples, the radiation damping time was taken from the results of Eq. (4) (see above), and a relative scale is used for the numerical value for the magnetization. Further, in contrast to the solutions to the regular Bloch equations with radiation damping, here, a boundary condition $M_z(0) = 0$ was used. This is due to the fact that initially, no sample is present in the NMR coil. The conditions of the simulation reasonably correspond to the actual hyperpolarized experiment. It can be seen from comparing Fig. 3c to the experimental results in Fig. 2c that the numerical solutions to Eqs. (5) and (6) qualitatively describe all of the features of the observed signal. Notably, there are multiple recurrences of signal of decaying amplitude, both with increased spacing, and of increased duration as time progresses. Furthermore, the longitudinal magnetization M_z is reduced after the last of the recurring signals.

The initial occurrence of signal, by the above equations, would depend on the amount of initially present transverse magnetization. Since this magnetization is presumably generated by random perturbations (noise) and is small, the observed signal occurrences may be expected to be irreproducible. Indeed, as stated above, the timing of signal occurrence varies from experiment to experiment. In the simulation, this is equivalent to a change in the relative magnitude of $M_T(0)$. In agreement with the narrow spectral region affected by radiation damping, the emissions of the two hyperpolarized spins in Fig. 2, from water and DMSO, appear to be independent. Finally, it should be noted that, similar to observations by Giraudeau et al. [5], if the ^{1}H nuclei are polarized to a positive spin temperature, and after injection and stabilization, the magnetization is inverted by a π-pulse followed by a pulsed field gradient, no signal recurrences were observed. Such a behavior would also be expected by the above model, as in this case only the spins that are within the NMR coil at the time of the pulse are inverted, and no additional negative polarization can be supplied. These conditions are therefore approximated by the solutions to Eqs. (2) and (3), which are represented in Figs. 3a and b.

In order to further confirm that introduction of fresh magnetization due to sample movement is the likely cause for the multiple beats of signal emission, experiments were carried out under varying injection conditions (Fig. 4). A trend is apparent, where an increased pressure differential for sample injection increases the number of recurrences of signal. The larger pressure differential gives rise to a larger amount of sample motion. The same is true for a variation in the height of the injection tube over the bottom of the NMR sample. Here, a lower height gives rise to a larger amount of turbulence [8,19]. Both of these observations provide support for a model, where sample replenishment leads to multiple signal emissions through radiation damping.

While an equation that fully describes the turbulent and inhomogeneous sample injection process would likely be impossible to write, it is remarkable that Eqs. (5) and (6), despite their simplicity, can capture most of the observed features of the signal. This includes the occurrence of multiple signals, the observation that these signals persist for a longer time, but appear less frequently at later points in time, and that their amplitude is decreasing. The functional form of the term used for introduction of the magnetization during the experiment was chosen as an exponential, in analogy to a physical relaxation process. It is possible, however, that this term underestimates the introduction of new sample at the beginning of the injection, and overestimates the residual motions of the sample at later times.

The observations presented here substantiate the notion that the process of introduction of a hyperpolarized sample, coupled with radiation damping gives rise to a complicated and perhaps unexpected behavior of the spin system. On a more practical level, the observation of the signal occurrences due to radiation damping in a ^{1}H spin system hyperpolarized to a negative spin temperature may be useful to judge the amount of residual turbulence after sample injection.

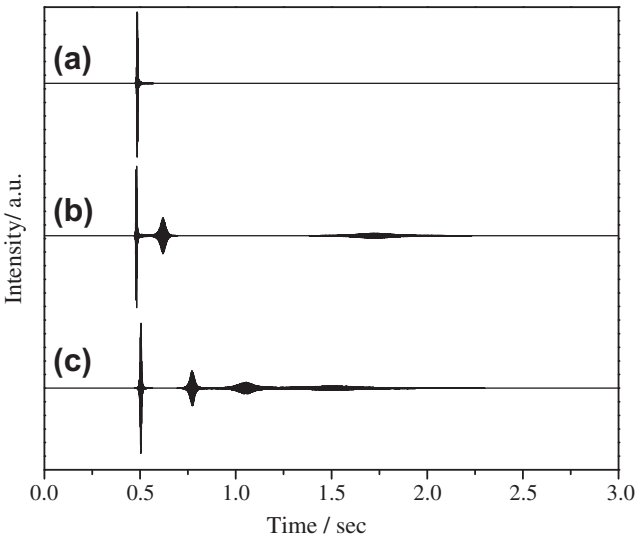

Fig. 4. Emissions of ^{1}H signal from mixtures of DMSO and D_2O (1:1 v/v) hyperpolarized to negative spin temperature, under varying conditions for injection of the sample into the NMR spectrometer. (a) "slow" injection with a differential pressure of 770 kPa and a tube height of 54 mm (tube height is the distance between the tip of the injection tube and the bottom of the NMR tube), (b) injection as in a, but with a tube height of 36 mm and (c) "fast" injection with a pressure differential of 820 kPa and a tube height of 30 mm.

4. Conclusions

Currently available commercial instrumentation is poised to make hyperpolarization readily accessible for routine spectroscopy, and a variety of approaches for efficient hyperpolarization are being developed. For example, it has been reported that ^{13}C polarization in some cases is more efficient at negative spin temperature [20]. In the case of ^{13}C polarization with small samples, radiation damping may not be an issue due to the lower overall magnetization. However, for spectroscopy with protons, the most abundant NMR active nuclei, as well as perhaps for NMR with probes exhibiting a high *Q*-factor, such as cryogenically cooled probes, this effect can become dominant. In the data shown here, the majority of the signal from a sample with negative spin-polarization is lost to radiation damping during sample injection, even before an NMR pulse can be applied. It is noted that in this case, the resonances affected by radiation damping stem from analytes at relatively low concentration ($\sim$100 mM), as opposed to highly abundant solvent species that would normally be the only ones expected to be subject to radiation damping. Such effects therefore need to be taken into account when working with hyperpolarized samples, and merit further exploration. The observations presented here also serve to demonstrate that when pursuing new applications of hyperpolarized NMR, even well-known effects such as radiation damping may give rise to highly unexpected behavior of the spin system.

Acknowledgments

Startup funds from Texas A&M University are gratefully acknowledged. CH thanks the Camille and Henry Dreyfus foundation for a new faculty award. Financial support was obtained from the National Science Foundation (Grant CHE-0846402) and from the Welch Foundation (Grant A-1658). SB was supported in part

by a fellowship from the Chemistry Biology Interface program administered by Texas A&M University.

References

[1] T. Sleator, E.L. Hahn, C. Hilbert, J. Clarke, Nuclear-spin noise, Phys. Rev. Lett. 55 (1985) 1742–1745.
[2] T. Sleator, E.L. Hahn, C. Hilbert, J. Clarke, Nuclear-spin noise and spontaneous emission, Phys. Rev. B 36 (1987) 1969–1980.
[3] M.A. McCoy, R.R. Ernst, Nuclear spin noise at room temperature, Chem. Phys. Lett. 159 (1989) 587–593.
[4] H. Desvaux, D.J.Y. Marion, G. Huber, P. Berthault, Nuclear spin-noise spectra of hyperpolarized systems, Angew. Chem. 121 (2009) 4405–4407.
[5] P. Giraudeau, N. Müller, A. Jerschow, L. Frydman, ^{1}H NMR noise measurements in hyperpolarized liquid samples, Chem. Phys. Lett. 489 (2010) 107–112.
[6] D.J.Y. Marion, G. Huber, P. Berthault, H. Desvaux, Observation of noise-triggered chaotic emissions in an NMR-maser, Chem. Phys. Chem. 9 (2008) 1395–1401.
[7] S. Reynolds, H. Patel, Monitoring the solid-state polarization of ^{13}C, ^{15}N, ^{2}H, ^{29}Si and ^{31}P, Appl. Magn. Reson. 34 (2008) 495–508.
[8] S. Bowen, C. Hilty, Rapid sample injection for hyperpolarized NMR spectroscopy, Phys. Chem. Chem. Phys. 12 (2010) 5766–5770.
[9] D.J.Y. Marion, H. Desvaux, An alternative tuning approach to enhance NMR signals, J. Magn. Reson. 193 (2008) 153–157.
[10] I.J. Day, J.C. Mitchell, M.J. Snowden, A.L. Davis, Applications of DNP–NMR for the measurement of heteronuclear T-1 relaxation times, J. Magn. Reson. 187 (2007) 216–224.
[11] H. Zeng, S. Bowen, C. Hilty, Sequentially acquired two-dimensional NMR spectra from hyperpolarized sample, J. Magn. Reson. 199 (2009) 159–165.
[12] J.H. Chen, B. Cutting, G. Bodenhausen, Measurement of radiation damping rate constants in nuclear magnetic resonance by inversion recovery and automated compensation of selective pulses, J. Chem. Phys. 112 (2000) 6511–6514.
[13] A. Abrgam, M. Goldman, Principles of dynamic nuclear polarisation, Rep. Prog. Phys. 41 (1978).
[14] R.A. Wind, M.J. Duijvestijn, C. van der Lugt, A. Manenschijn, J. Vriend, Applications of dynamic nuclear-polarization in ^{13}C NMR in solids, Prog. Nucl. Mag. Res. Sp. 17 (1985) 33–67.
[15] X.A. Mao, D.H. Wu, C.H. Ye, Radiation damping effects on NMR signal intensities, Chem. Phys. Lett. 204 (1993) 123–127.
[16] W.S. Warren, S.L. Hammes, J.L. Bates, Dynamics of radiation damping in nuclear magnetic resonance, J. Chem. Phys. 91 (1989) 5895–5904.
[17] D.J.Y. Marion, P. Berthault, H. Desvaux, Spectral and temporal features of multiple spontaneous NMR-maser emissions, Eur. Phys. J. D 51 (2009) 357–367.
[18] M.G. Richards, B.P. Cowan, M.F. Secca, K. Machin, The ^{3}He nuclear Zeeman maser, J. Phys. B-At. Mol. Opt. 21 (1988) 665–681.
[19] S. Bowen, C. Hilty, Time-resolved dynamic nuclear polarization enhanced NMR spectroscopy, Angew. Chem. Int. Ed. 47 (2008) 5235–5237.
[20] M.G. Saunders, C. Ludwig, U.L. Günther, Optimizing the signal enhancement in cryogenic ex situ DNP–NMR spectroscopy, J. Am. Chem. Soc. 130 (2008) 6914–6915.